Combustion Characteristics of Methanol Fueled Carburettor Engines

COMBUSTION CHARACTERISTICS OF METHANOL FUELED CARBURETTOR ENGINES

Shigenobu Hayashi and Norihiro Sawa*

Abstract

Methanol, which contains oxides, is investigated as fuel for internal combustion engines. If methanol is used as fuel in internal combustion engine, consequently, there is a large possibility to reduce the NO_x concentration without lowering the engine power.

However, the combustion characteristics of methanol in the cylinder remain almost unknown to be solved in the future.

Therefore, the authors carried out researches on the influence of operating conditions on the engine power, combustion and exhaust-gas characteristics, furthermore, on the rate of effective heat release and the mass rate of burning, and so on.

1. Introduction

Methanol, which contains oxides, can be comparatively easily burnt in a from of lean mixture, increase the compression ratio because of its high octane number and has a comparatively low burning temperature because of the high latent heat of the fuel itself. If methanol is used as fuel in internal combustion engines, consequently, there is a large possibility to reduce the NO_x concentration without lowering the engine power. Also as an energy source replacing gasoline, moreover, it has attracted special interests recently and is investigated from the standpoint of fuel for internal combustion engines[1]~[3]. However, the combustion characteristics of methanol are almost unknown. Therefore, the authors carried out researches on the following points :

Influence of operating conditions on the engine power and exhaust-gas characteristics (CO, THC, NO_x and RCHO concentrations); As characteristics representing the combustion, an average value $\bar{P}_{max}$, the standard deviation S and the coefficient of variation $S/\bar{P}_{max}$, of the maximum combustion pressure P_{max} ; Correlation between $\bar{P}_{max}$ and its appearance period $\theta(\bar{P}_{max})$; Rate of effective heat release ; Mass rate of burning etc.

2. Experimental Apparatus and Methods

2. 1 Experimental apparatus

For the experiment, the authors used a water-cooled, single-cylinder and overhead-valve engine and an air-cooled, single-cylinder and side-valve engine but the former more frequently. Specifications of these engines are as shown in Table 1. The experimental apparatus is composed of a unit for measuring the breathing air (surge tank 4, round nozzle 1, thermometer 3 and manometer 2), a fuel feed system (fuel tank, fuel flow meter 7, carburettor

* : Professor, Dr., Dept. of Mechanical Engineerings,
Faculty of Engrs. Ibaraki University, Narusawa-cho, Hitachi

Table.1 Specifications of test engine

Engine / Specification	E-482 (OHV type)	E-252 (SV type)
Cylinder bore × Stroke mm	φ85 × 85	φ72 × 62
Stroke volume cc	482	252
Compression ratio	8.4	6.4
Rated horsepower	6 Ps/2000 rpm (ε = 4.8)	4.7 Ps/3600 rpm

Table.2 Operating condition of test engine (E-482)

Engine speed		2000 rpm
Ignition advance		23.5, 35, 48.5 (°CA)
Volumetric efficiency		26.5, 42.5, 63 (%)
Intake pipe wall temperature		9, 44, 53 (°C)
Water content of fuel	y = methanol	0, 0.25, 0.5 (%)
	y_g = gasoline	0, 0.5, 1.0 (%)

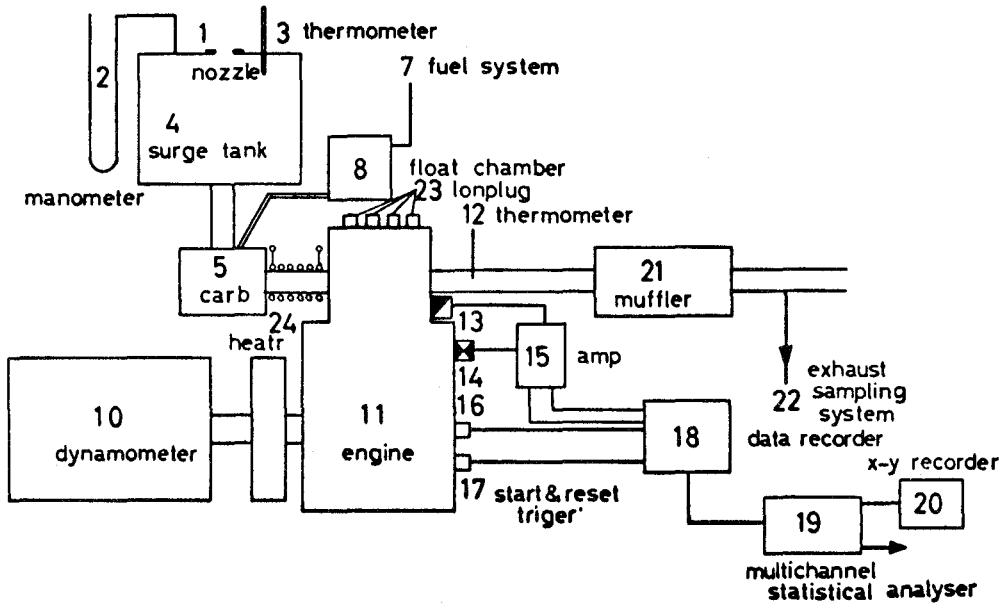

Fig. 1 : Schematic diagram of experimental apparatus

float chamber and carburettor body 5), a suction pipe system (pipe wall heater 24 and pipe wall thermometer 25), the tested engine 11, an exhaust pipe system (exhaust thermometer 12, muffler 21 and exhaust gas extracting oriffice 22) and a dynamometer 10.

To investigate the combustion state, further, strain gauge type pressure indicators 13 are used, in the case of the side-valve engine ion plugs 23 are connected to the cylinder head in order to detect the flame velocity and start trigger pulse marker 16, reset pulse marker (to top dead center marker) etc. to allow the use of statistical data processor 19.

The concentrations of carbon monoxide CO, nitrogen oxides NO_x, total hydrocarbons THC and aldehyde RHCO in the exhaust gas are determined with nondispersive infrared analyzer, by the zinc-reduced naphthyle thylene diamine method[4], with FID gas-chromatograph and the Kitagawa's detector tube No.71 for formaldehyde, respectively. For this purpose, the exhaust gas extracting pipe is heated with a ribbon heater so as to eliminate possible influence of the water content.

2. 2 Experimental methods

At first, each of the tested engines is stationarily operated for about ten minutes under the conditions as shown in Table 2 while the engine speed N and the volumetric efficiency η_v being fixed at 2000rpm and 42.5%, respectively. After the flow rate of fed fuel is regulated by adjustment of vertical position of the float chamber, then, the power L_e, fuel flow rate G_f, the exhaust gas temperature t_e, the concentrations of CO, NO_x, THC, RHCO etc. are measured for various values from 0.7 to 1.5, of the excess air ratio λ. At the same time, the cylinder combustion pressure, top dead center mark etc. are indicated on a data recorder, these values are reproduced and fed to the statistical data processor, which draws variation frequency curves of the combustion pressure at each crank angle, average pressure diagram at 1000 cycle etc.

3. Experimental Results and Considerations

3. 1 Characteristics of power and exhaust emission

The influences of the excess air ratio λ and suction pipe wall temperature t_w on the engine power and exhaust emission under methanol operations as well as comparison of them with those under gasoline operations (solid line, $y_g=0$) are shown in Figs.2 and 3, the influence of the water content y under water-containing methanol operations in Fig.4 and that of the ignition advance angle θ shown in Fig.5. In each of these figure, only one example is indicated. As can be seen from them.

1) Within a rich mixture range, $\lambda=0.6$ to 1.0, the engine power L_e and the thermal efficiency η under methanol operations are higher than those under gasoline operations, respectively (Figs.2 and 3) and increase, though slightly, further under water-containing methanol operations (Fig.4). In addition, L_e and η increase on the whole with the increasing ignition advance θ (Fig.5). In either case, lean mixture makes the heat release decrease and at the same time the combustion conditions deteriorate so that L_e and η are decreased.

However, the higher suction pipe wall temperature t_w, the lower water content y and the larger ignition advance θ improve L_e and η, resulting also in the wider combustible range.

If methanol evaporation is promoted (for example, 100% of methanol evaporates for $\lambda=1$ and at $t_w=44$℃) by heating the suction pipe, in particular, their improvement at the lean mixture side is remarkable.

2) The carbon monoxide concentration CO depends mainly on the excess air ratio λ and within a lean mixture range, $\lambda>1.1$, it does not almost depend on whether the engine is operated with gasoline or methanol as well as on the operating conditions such as the suction pipe wall temperature t_w, water content y, ignition advance θ etc. to be about 0.2 to 0.3%.

Within a rich mixture range, $\lambda<1.0$, the CO concentration increases with decreasing λ. At the same value of λ, the concentration increases with decreasing t_w (Fig.2), increasing y (Fig.4) and decreasing θ (Fig.5) and its value under methanol operations is, though slightly, lower than that under gasoline operations (comparison of dotted line with ● marks in Figs.2 and 3). As can be guessed from calculation results of the chemical equilibrium formula, it appears that the above-mentioned decrease in CO concentration is caused by the lowering of combustion temperature (comparison of $K_w=4$ with $K_w=1$ in Fig.3) and the difference in fuel

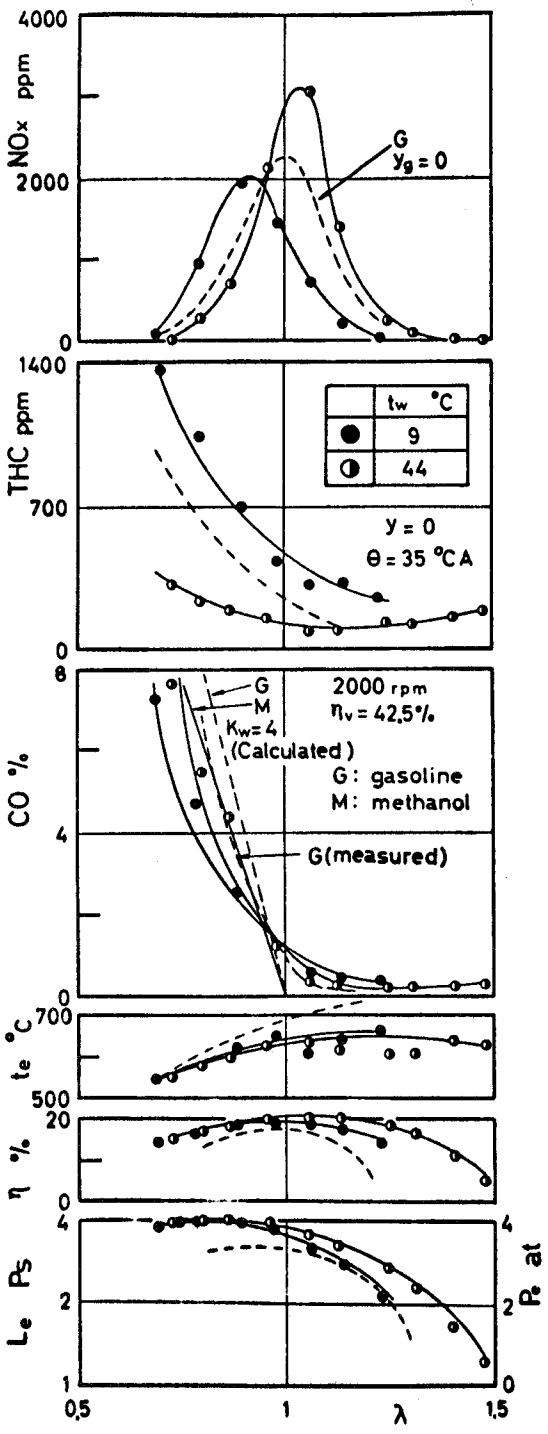

Fig. 2 : Engine power, exhaust emissions vs. excess air ratio λ

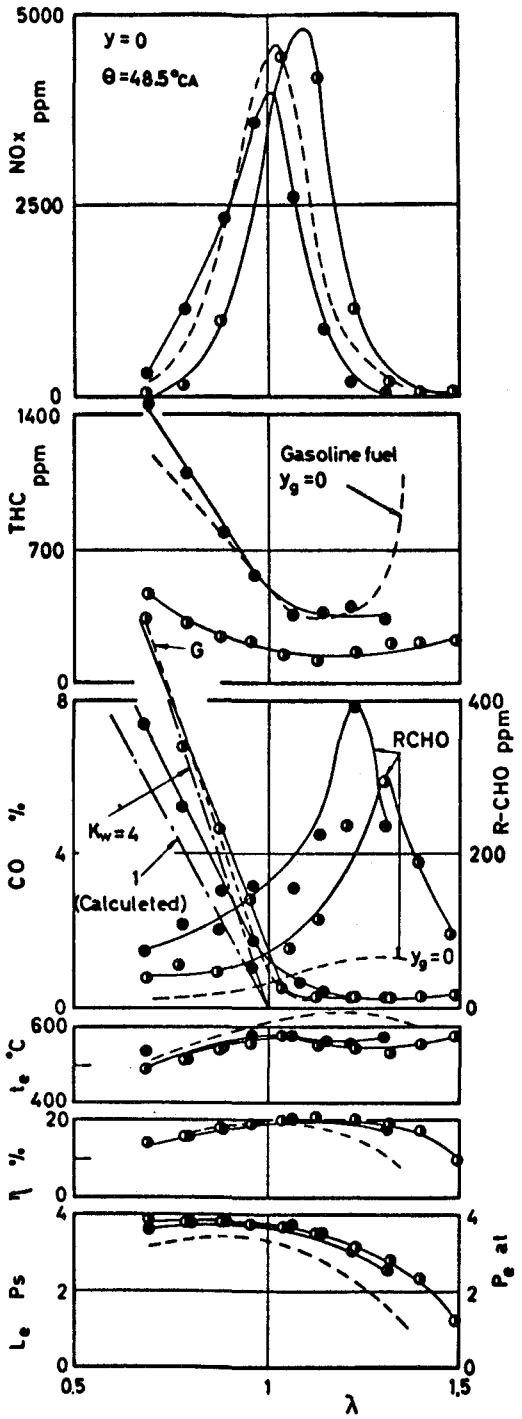

Fig. 3 : Engine power, exhaust emissions vs. excess air ratio λ, Mark G : gasoline, M : methanol

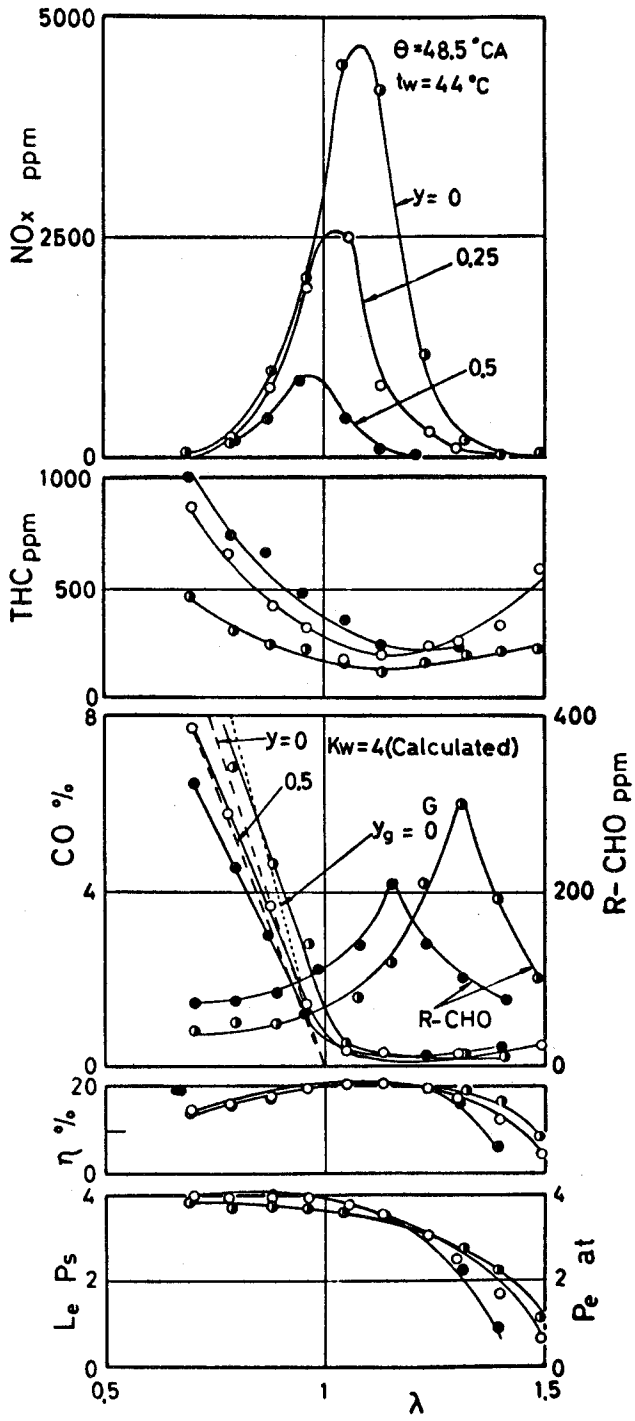

Fig. 4 : Engine power, exhaust emissions vs. water content y

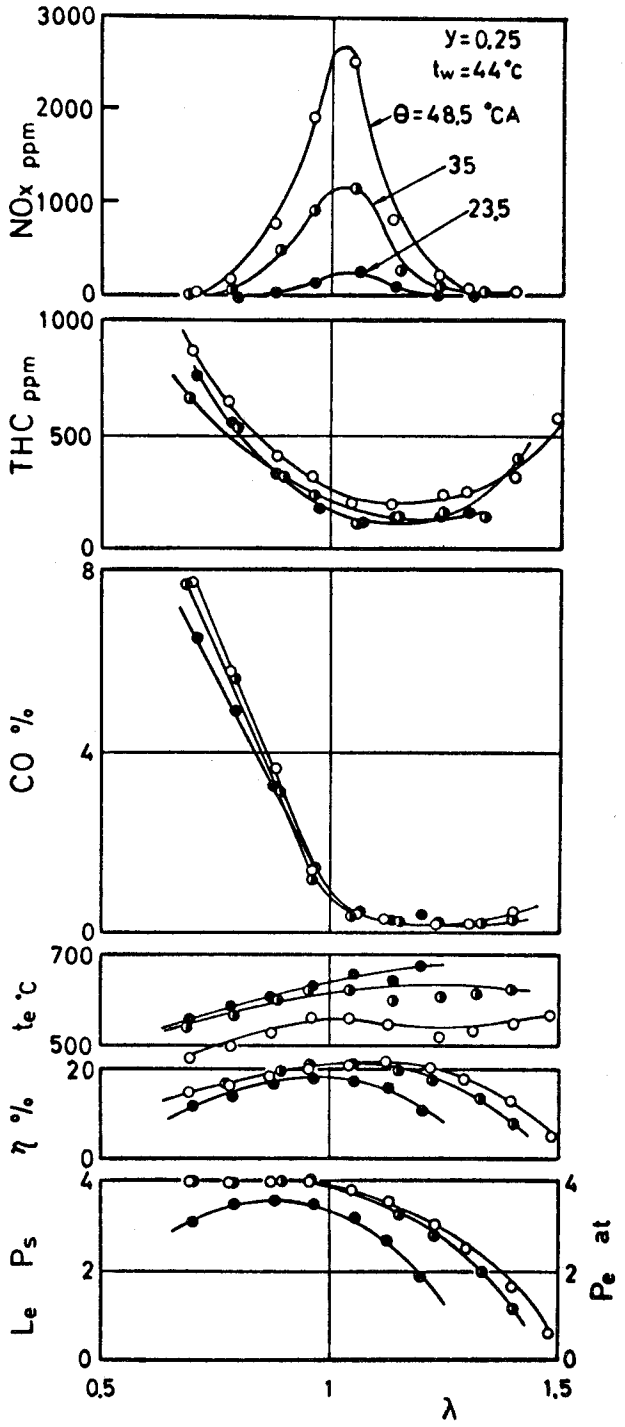

Fig. 5 : Engine power, exhaust emissions vs. ignition advance θ

composition (comparison between M and G lines in Fig.2).

3) In all cases, the total hydrocarbon concentration THC have respective minimal near $\lambda=$ 1.1 to 1.2 and increase either at higher or at lower side than this range. Since in this case methanol does not so actively evaporate in the suction pipe as gasoline, the THC concentration under methanol operations is considerably higher than that under gasoline operations unless the suction pipe is heated. If the pipe heated, on the contrary, the mixture becomes more uniform and the quantity of fuel adhering to the cylinder wall decreases so that the THC concentration decreases on the whole to be lower than its value under gasoline operations. Since, if the water content y is higher, evaporation of the fuel becomes worse, the mixture becomes less uniform and in addition the combustion temperature drops, so that the THC concentration increases (Fig.4). If the ignition timing is made to advance, the combustion temperature rises but on the contrary the combustion period θ_b is shorter and gas temperature in the latter half of the expansion stroke or in the exhaust pipe after opening of the exhaust valve falls, so that the oxidation reaction of unburned hydrocarbon proceeds more slowly and consequently the variation in THC concentration is slighter (Fig.5).

4) The aldehyde concentration RCHO under meteanol operations is considerably higher than that under gasoline operations ($y_g=0$ in Fig.3). This is perhaps caused by a fact that under the latter, methane formed by thermal decomposition in the quench area is oxided to from formaldehyde, whereas under the former operations, formaldehyde is directly formed, by thermal decomposition and oxidation reaction, more easily.

5) The nitrogen oxides concetration NO_x under methanol operations is lower, to some degree, than that under gasoline operations. If the suction pipe wall temperature t_w is raised (Fig.2) and the ignition advance θ increased (Fig.5), however, the NO_x concentration is increased and becomes higher than that under gasoline operations. If the water content y is increased (Fig.4), on the other hand, decrease of the combustion temperature due to increase in latent heat of fuel makes NO_x remarkably decrease. Moreover, all the conditions which decrease NO_x tend to lower the engine power within the lean mixture range. Consequently, it is necessary to select the most suitable values of t_w, y, θ etc. without lowering engine power. On the basis of the engine power $L_e=3.3$ Ps at $\lambda=1$ under gasoline operations ($\theta=$ 35°CA and $\eta_i=42.5\%$), now, let us compare the value of the thermal efficiency η and the exhaust emission concentrations : under gasoline operations, $\eta=20\%$, CO=0.7%, THC= 260ppm, RHCO=25ppm and $NO_x=2400$ppm, whereas under methanol operations ($\theta=48.5$ °CA, y=0.5 and $t_w=44$°C), $\eta=18\%$, CO=0.6%, THC=200ppm, RHCO=120ppm and $NO_x=$ 130ppm. Although η decreases by 2%, that is, not only CO and THC but also NO_x are reduced and the reduction of NO_x is particularly remarkable, amounting to about 1/20. While RCHO should be reduced by means of a suitable method, it is possible to decrease further CO, THC etc. by heating the suction pipe. If the water-containing methanol is used and measures to promote its evaporation are taken, consequently, it may be a very useful fuel for carburettor engine.

3.2 Cycle-by-cycle variation of combustion pressure

3.2.1 Frequency of combustion pressur variation

Figs.6, 7 and 8 show the average pressure diagram (F vs. θ) at 1000 cycle, the variation frequencies F % of the combustion pressure P at 5.6 and 1.6 °CA before and 8.8 and 16 °CA after the top dead center (TDC) and the maximum combustion pressure $\overline{P}_{max}$. Combustion variation at the initial stage of the combustion process depends essentially on ignition lag and the condition of mixture near the ignition plugs, whereas pressure variation is more amplified when the mass rate of burning is larger. If the excess air ratin is higher, the suction pipe wall temperature lower and water content larger, for this reason, the ignition lag more increases and moreover the flame velocity V_f also decreases, so that the mass rate of burning at the same crankangle before the TDC decreases. As shown in the figures, consequently, the pressure variation decreases with increasing λ (Fig.6), decreasing t_w and increasing y (Fig.7). A similar phenomenon can be observed also when the ignition advance θ is decreased. Since fuel perfectly evaporates in the combustion process after the TDC and the mixture also becomes uniform, the process depends on the average propertied of mixture and it is affected by the variation of average mixture ratio but since lower combustion before the TDC makes larger the mass rate of burning, the pressure variation in this period also increases. The variation of the maximum combustion pressure $\overline{P}_{max}$, so far frequently used for representing combustion variation, is similar to that of the combustion pressure at a crank angle after the TDC, because the maximum pressure is produced after the top dead center.

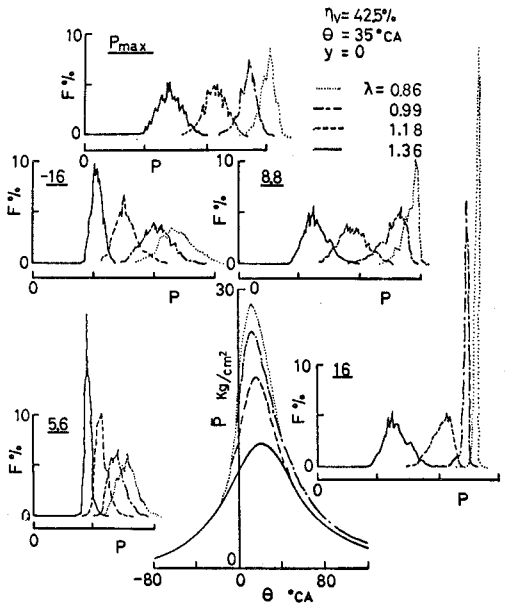

Fig. 6 : Frequency of cylinder pressure variation F vs. excess air ratio λ

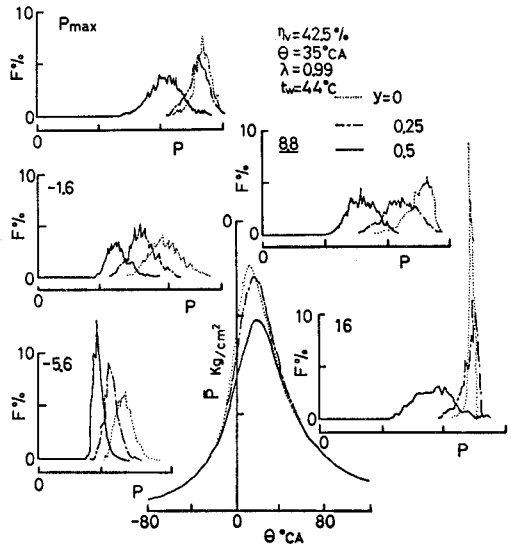

Fig. 7 : Frequency of cylinder pressure variation F vs. water content y

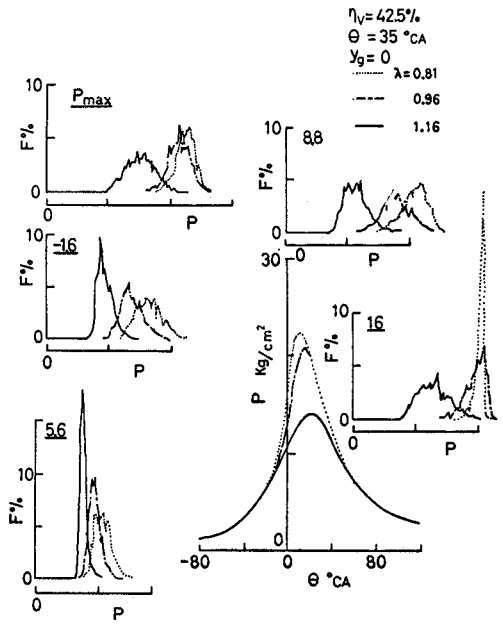

Fig. 8 : Frequency of cylinder pressure variation F vs. excess air ratio λ (gasoline fueled engine)

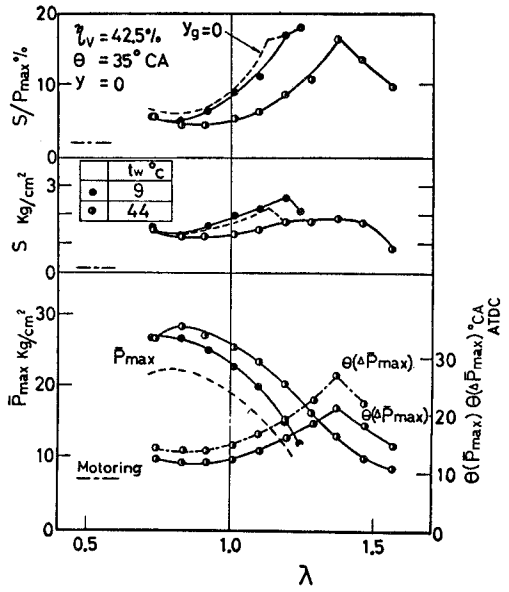

Fig. 9 : Combustion characteristics vs. excess air ratio λ and temperature of intake pipe wall t_w

For this reason, it cannot be said that the variation of $\bar{P}_{max}$ represents precisely that of the combustion as a whole but since the former is closely related to combustion condition during the so-called principal combustion period after the TDC and also deeply connected with the combustion noise and the RHCO concentration, it can be a useful index indicating the combustion condition. Such pressure variation frequency distribution curves are perfectly the same in either case of methanol and gasoline operations.

3.2.2 Variation of maximum combustion pressure

Simultaneously with the experiments shown in Figs.2 to 5 the cylinder combustion pressure is recorded, based on these results the average maximum combustion pressure $\bar{P}_{max}$, its forming period θ ($\bar{P}_{max}$), the standard deviation S of P_{max}, the coefficient of variation $S/\bar{P}_{max}$ etc. are determined and given in Figs.9, 10 and 11. And, as an example of the experimental results obtained on the side-valve engine, Fig.12 shows $\bar{P}_{max}$, $\theta(\bar{P}_{max})$, the maximum $\Delta\bar{P}_{max}$ of a difference $\Delta\bar{P}$ between the combustion and motoring pressures, its forming period $\theta(\Delta\bar{P}_{max})$, the combustion duration θ_b and the flame velocity V_f (1 to 2) and V_f (1 to 3) calculated from the time when flame passes through the ion plugs 1 to 2 and 1 to 3. As can be seen from the figures, evaporation of methanol in the suction pipe is comparatively bad and for this reason the mixture is not uniform with its large variation. When the suction pipe wall temperature t_w is 9 °C (● marks in Fig.9), consequently, the deviation S of P_{max} is larger, to some degree, than that under gasoline operations (dotted line in Fig.9). Since the calorific value of methanol mixture is larger than that gasoline mixture and in proportion to this $\bar{P}_{max}$ also higher, however, the coefficient of variation $S/\bar{P}_{max}$ under methanol operations

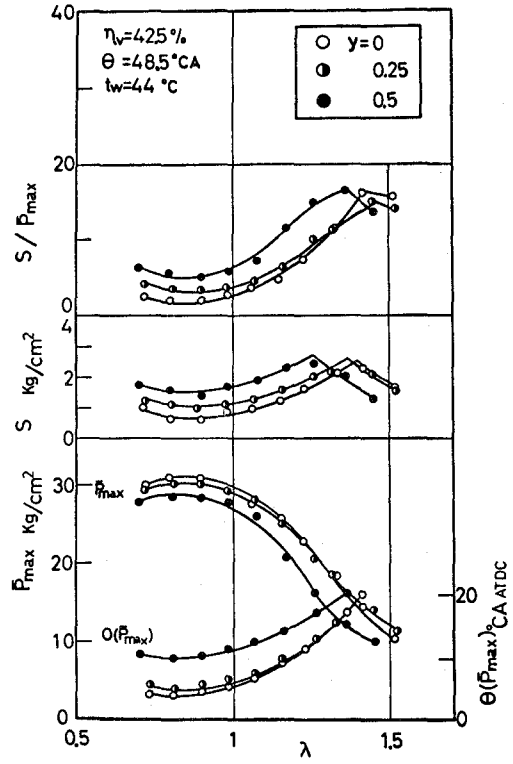

Fig. 10 : Combustion characteristics vs. water content y

is slightly lower than that under gasoline operations. On the other hand, $\bar{P}_{max}$ increases with increasing t_w (OEP in Fig.9), decreasing water content y (Fig.10) and increasing ignition advance θ (Fig.11), at the same time the forming period of $\bar{P}_{max}$ approaches the TDC, that is, $\theta(\bar{P}_{max})$ decreases and S as well as $S/\bar{P}_{max}$ also decrease. Since in either case the flame velocity is the highest near $\lambda=0.85$, then $\theta(\bar{P}_{max})$ becomes minimum, $\bar{P}_{max}$ maximum, and S as well as $S/\bar{P}_{max}$ are minimum. Since v_f decreases with increasing λ, however, $\theta(\bar{P}_{max})$ increases, $\bar{P}_{max}$ decreases and S as well as $S/\bar{P}_{max}$ also increase. When λ exceeds certain value, S and $S/\bar{P}_{max}$ on the contrary decrease. There is a positive correlation between $S/\bar{P}_{max}$ and $\theta(\bar{P}_{max})$, because this $S/\bar{P}_{max}$ versus λ curve is similar to the $\theta(\bar{P}_{max})$ versus λ. $S/\bar{P}_{max}$ under motoring operations is 2 %, in each of the engines tested there is a variation, in charged fresh air, of this order and it appears that P_{max} is caused to change as a result of synergistic effect of a combustion variation related to the mixture with the above-mentioned. In the case of firing operations, the minimum values of $S/\bar{P}_{max}$ are 6 %, 5 % (t_w=9 °C) and 4 % (t_w=44 °C) under operations with gasoline and methanol and when the suction pipe is heated, respectively.

Even if the operating condition is altered, it is considerably difficult to improve $S/\bar{P}_{max}$. This $S/\bar{P}_{max}$ increases with increasing λ and attains, e.g., 17 % (t_w=9 °C) at λ=1.2.

If the suction pipe is heated, however, $S/\bar{P}_{max}$ is remarkably improved to be decreased down to 9 % (t_w=44 °C).

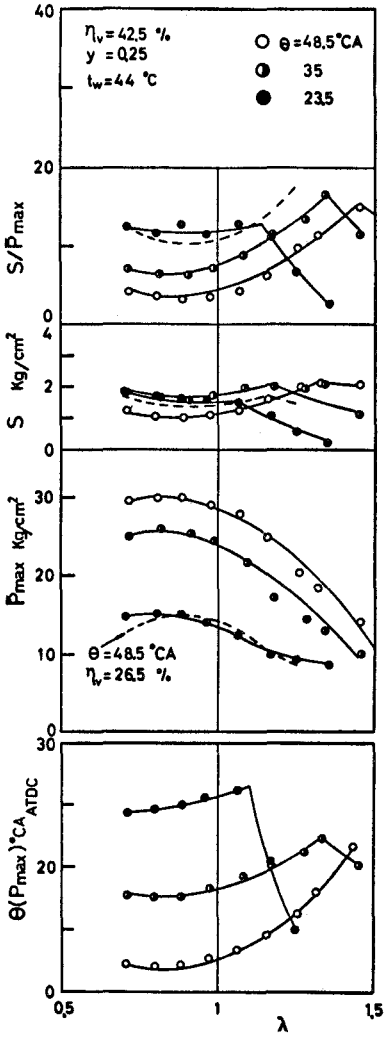

Fig. 11 : Combustion characteristics vs. ignition advance θ

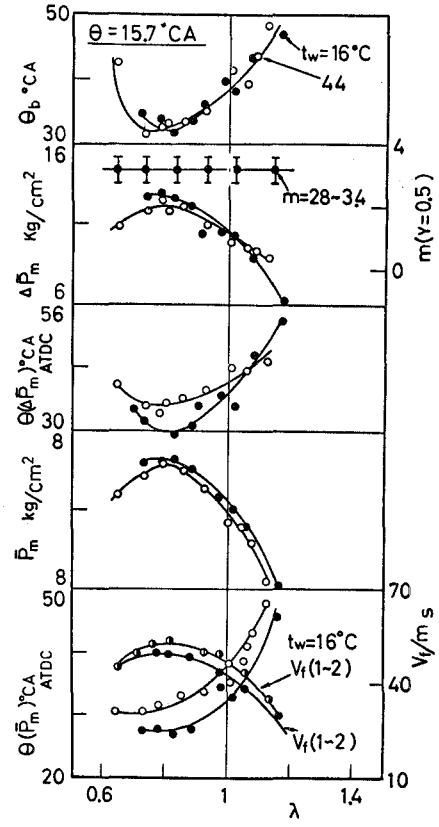

Fig. 12 : Combustion characteristics vs. excess air ratio λ (side valve type engine E-252)

The improving effect due to suction pipe heating is thus more remarkable under conditions of more difficult combustion.

3. 3 Correlation between the combustion characteristics

3. 3. 1 Maximum cylinder pressure $\bar{P}_{max}$

Various correlations among the mean maximum combustion pressure $\bar{P}_{max}$, its forming preiod θ ($\bar{P}_{max}$), the maximum value $\Delta\bar{P}_{max}$ of a difference $\Delta\bar{P}$ between the mean combustion $\bar{P}$ and compression $\bar{P}_c$ pressures are shown in Figs. 13, 14 and 15.

According to these figures, there is a linear correlation between $\bar{P}_{max}$ and $\Delta\bar{P}_{max}$ (Fig. 13) and all the points lie on the same gradient line, which does not depend on whether the side-valve engine E-252 (SV) or a two-cycle (H) is tested, on whether a tested engine is

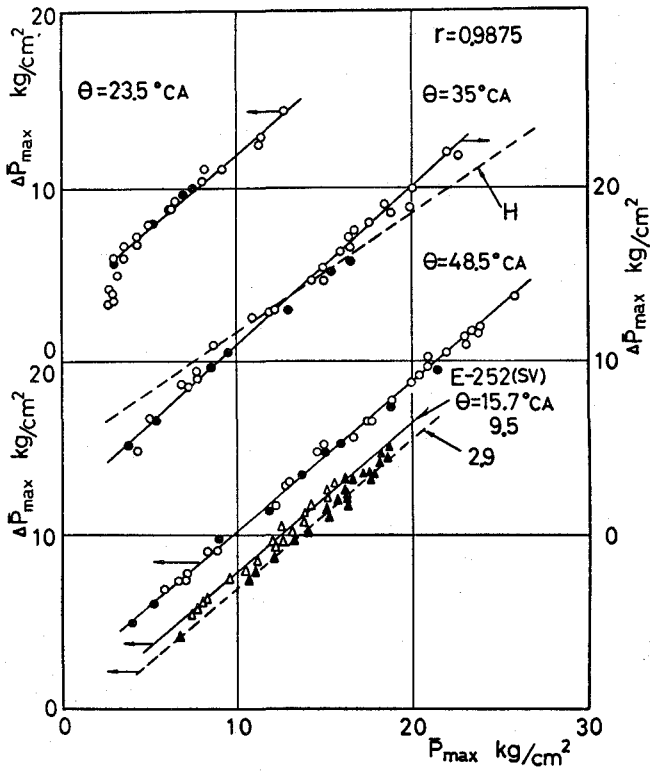

Fig. 13 : Correlation between $\Delta\bar{P}_{max}$ and $\bar{P}_{max}$

operated with methanol (○mark) or gasoline (● mark) and on operating conditions such as the suction pipe wall teperature etc. The forming periodos of $\bar{P}_{max}$ and $\Delta\bar{P}_{max}$ correspond to a condition where flame spreads sufficiently in the combustion chamber and depend mainly on such average properties as mixture ratio and charged quantity of fresh air in the combustion chamber. If the breathing air and the engine speed are kept constant irrespective of the operating conditions as the present experiment, consequently, it appears that a particularly strong correlation (coefficient of correlation γ=0.9875) exists between $\bar{P}_{max}$ and $\Delta\bar{P}_{max}$. If the combustion velocity is larger and the combustion completed in an early stage, that is, $\theta(\Delta\bar{P}_{max})$ is shorter, $\bar{P}_{max}$ and $\Delta\bar{P}_{max}$ are formed while the combustion chamber having only a smaller volume, whith lower heat loss, so that the values of $\bar{P}_{max}$ and $\Delta\bar{P}_{max}$ becom both larger.

As shown in Figs. 14 and 15, consequently, strong negative correlations exist between $\bar{P}_{max}$ and θ ($\bar{P}_{max}$) as well as between $\Delta\bar{P}_{max}$ and θ ($\Delta\bar{P}_{max}$), respectively. When λ increases and $S/\bar{P}_{max}$ rapidly decreases, however, θ ($\bar{P}_{max}$) also decreses in this range ($\lambda > 1.3$ to 1.4) so that within the range there exists on the contrary a positive correlation between $\bar{P}_{max}$ and $\theta(\bar{P}_{max})$.

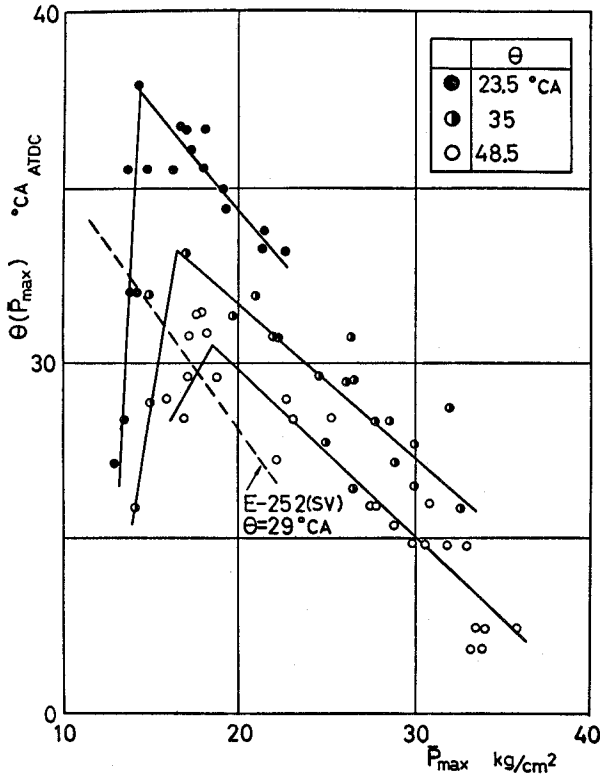

Fig. 14 : Correlation between $\theta(\bar{P}_{max})$ and $\bar{P}_{max}$

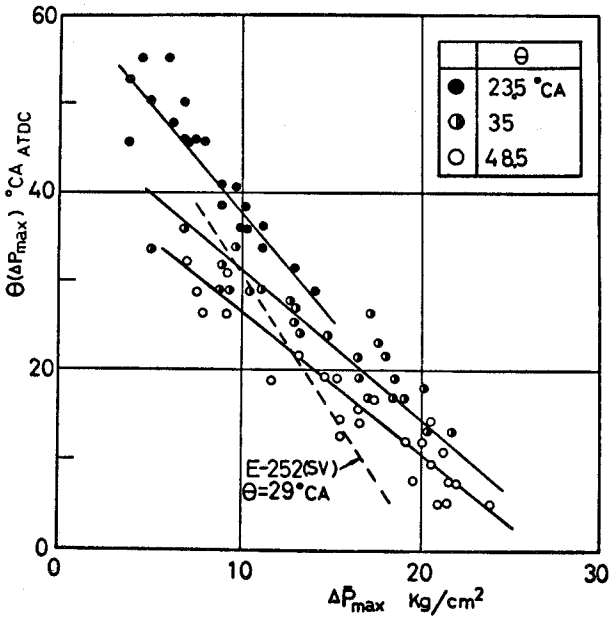

Fig. 15 : Correlation between $\theta(\Delta\bar{P}_{max})$ and $\Delta\bar{P}_{max}$

Although a similar correlation can be observed also when the ignition advance θ is altered, $\bar{P}_{max}$ and $\Delta\bar{P}_{max}$ decrease as well as θ ($\bar{P}_{max}$) and θ ($\Delta\bar{P}_{max}$) increase with decreasing θ, so that it is impossible to make the experimental results lie on one straight line. Since correlations exist between $\bar{P}_{max}$ and $\Delta\bar{P}_{max}$, between $\bar{P}_{max}$ and θ ($\bar{P}_{max}$) and between $\Delta\bar{P}_{max}$ and θ ($\Delta\bar{P}_{max}$), a positive correlation must exist also between θ ($\bar{P}_{max}$) and θ ($\Delta\bar{P}_{max}$).

3. 3. 2 Maximum heat release

Fig. 13 shows a representative result of the mass rate of burning $Y=\Delta\bar{P}/\Delta\bar{P}_{max}$, calculated by the Rassmeiler's method [5] from the average combustion $\bar{P}$ and compression $\bar{P}_c$ pressures at 1000 cycle. Z on the abscissa is a ratio of the crank angle θ from combustion start to the combustion period θ_b, that is, $Z=\theta/\theta_b$ and the combustion start and end correspond to moments when the cylinder pressure begins to become higher than the motoring and when $\Delta\bar{P}$ becomes equal to $\Delta\bar{P}_{max}$. According to such a result of analysis as this, the combustion becomes slower (with slower increase in $\Delta\bar{P}$) with increasing excess air ratio λ and water content y and decreasing suction pipe wall temperature t_w and ignition advance θ, so that the period of combustion end $\theta(\Delta\bar{P}_{max})$ is delayed and $\Delta\bar{P}_{max}$ also lowered. An equation of this mass rate of burning is given by Wiebe as follows[6] :

$$Y=1-e^{-az^{m+1}} \quad \cdots\cdots (1)$$

where $\underline{a}$ and $\underline{m}$ denote characteristics numbers on combustion and Wiebe described that $\underline{a}=6.9$, $\underline{m}=0.1$ to 1.0 for diesel engine and 1.0 to 3.0 for gasoline engine. However, the results obtained in the present experiment under both gasoline (○ mark) and methanol (● mark) operations do not coincide with the Wiebe's calculation curve (Fig. 13), that is, it shows such a condition that $\underline{m}$ is lower at the initial stage of combustion and becomes large towards final stage. Now, let us determine an average value of $\underline{m}$. Read the value of Z at $Y=0.5$ out of the Y versus z curve and after substituting it into Eq. (1) calculate the value of $\underline{m}$ backwards, then, although the value of $\underline{m}$ depends to some degree on λ, t_w, θ etc., it is kept within a range from 2.5 to 4.3 (see Fig. 12). With Y denoting the mass rate of burning, the rate of heat release is given, from the Wiebe's formula (1), by the following :

$$\frac{d\bar{Q}}{d\theta}=H_u\cdot G_f\cdot\frac{dY}{d\theta}=H_u\cdot G_f\cdot e^{-az^{m+1}}\cdot a(m+1)\frac{z^m}{\theta_b} \quad \cdots\cdots (2)$$

Differentiate Eq. (2) with θ and put $\frac{d\bar{Q}}{d\theta}=0$, then $z=\left[\frac{1}{a(m+1)}\right]^{1/(m+1)}$, which is a condition for $\frac{d\bar{Q}}{d\theta}$ to maximum.

Consequently, the maximum value of heat release $\left(\frac{d\bar{Q}}{d\theta}\right)_{max}$ is

$$\left(\frac{d\bar{Q}}{d\theta}\right)_{max}=\frac{H_u\cdot G_a/M_o}{\lambda\,\theta_b}\cdot\underline{a}(\underline{m}+1)\{\underline{m}/\underline{a}(m+1)\}^{\underline{m}/(\underline{m}+1)}e^{-\underline{m}/(\underline{m}+1)} \quad \cdots\cdots (3)$$

where H_u: The lower calorific value of fuel, G_f: Flow rate of the fuel, G_a: Quantity of breathing air, λ: Excess air ratio, Mo : Theoretical air/fuel ratio, θ_b: Duration of combustion, $\underline{a}$ and $\underline{m}$: Characteristics numbers on the combustion.

Since, in the present experiment, G_a is constant, the experimental value of $\underline{m}$ is 2.5 to 4.3

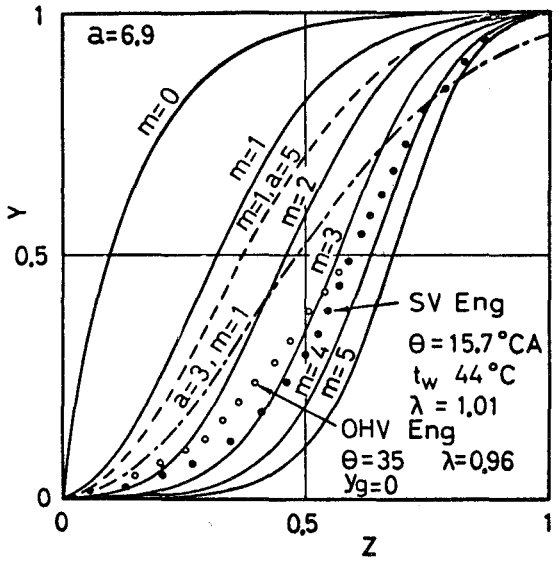

Fig. 16 : Burning mass rate Y and Wiebe's function

and the corresponding value of $a(m+1)\cdot\{m/a(m+1)\}\cdot e^{-m/(m+1)}$ 2.3 to 2.8 provided that $\underline{a}=$ 6.9, on the assumption that this value is also constant, the value $\left(\frac{d\bar{Q}}{d\theta}\right)_{max}$ is proportional to $(H_u/M_o)/(\lambda\theta_b)$. From the equation of energy equilibrium for mixture in the cylinder as well as that of state for gas, on the other hand, the rate of heat release is given by

$$\frac{d\bar{Q}}{d\theta}=\frac{A}{\kappa-1}\left(\kappa\cdot\bar{p}\frac{dV}{d\theta}+V\frac{d\bar{P}}{d\theta}\right)+\frac{d\bar{Q}_W}{d\theta} \quad \cdots\cdots (4)$$

where $\bar{Q}$: Quantity of heat release, $\bar{Q}_w$: Quantity of emitted heat, θ: Crank angle, A: Heat equivalent of work, κ: Specific heat ratio of mixture in the cylinder, $\bar{P}$: Average combustion pressure at 1000 cycle, V: Volume of the combustion chamber.

If successive numerical calculation of Eq.(4) is carried out with the average pressure diagram, consequently, it is possible to obtain easily an effective rate of heat release $\left(\frac{d\bar{Q}}{d\theta}-\frac{d\bar{Q}_w}{d\theta}\right)$. While an empirical formula on $(d\bar{Q}_w/d\theta)$ is proposed, Fig. 17 shows a relation between $(H_u/M_o)/(\lambda\theta_b)$ and $\left(\frac{d\bar{Q}}{d\theta}-\frac{d\bar{Q}_w}{d\theta}\right)_{max}$ which is calculated instead of $(d\bar{Q}/d\theta)_{max}$ because $d\bar{Q}_w/d\theta$ is proportional to $d\bar{Q}/d\theta$ and its value is comparatively small. From the figure, it can be seen that the experimental values either case of methanol (○ mark) and gasoline (● mark) operations lie well on a straight line and, for this reason, that there exists a strong positive correlation ($\gamma=0.9584$) between $\left(\frac{d\bar{Q}}{d\theta}\right)_{max}$ and $(H_u/N_o)/(\lambda\theta_b)$.

Since as mentioned in the preceding section $\bar{P}_{max}$ increases with decreasing combustion period θ_b, $\bar{P}_{max}$ is proportional to $1/\lambda\theta_b$. Consequently, a positive correlation ($\gamma=0.9225$) exists also between $\left(\frac{d\bar{Q}}{d\theta}\right)_{max}$ and $\bar{P}_{max}$ (Fig. 18).

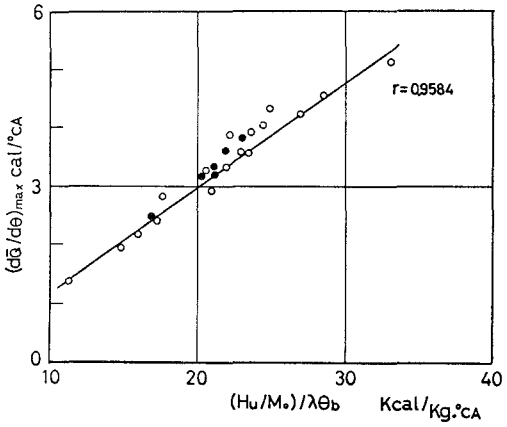

Fig. 17 : Correlation between $(d\bar{Q}/d\theta)_{max}$ and $(H_u/M_o)/\lambda\theta_b$

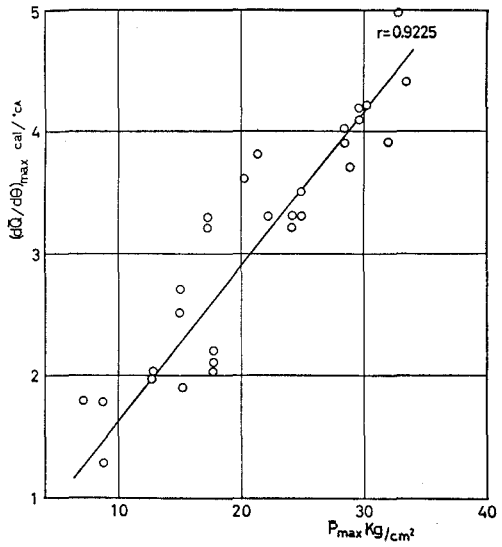

Fig. 18 : Correlation between $(d\bar{Q}/d\theta)_{max}$ and $\bar{P}_{max}$

4. Conclusion

The influences of methanol-operating conditions of four-cycle spark-ignition engine on the engine power, the characterisitics of exhaust gas and combustion variation were investigated experimentally besides the correlation among combustion characteristics. The obtained results can be summarized as follows :

1) Since methanol evaporates only inactively in the suction pipe because of its large latent heat, it is necessary to promote evaporation by heating the suction pipe wall makes the concentration of total hydrocarbon THC decrease but on the contrary that of nitrogen oxides NO_x increase. Although it is possible to lower NO_x by means of operating with lean mixture, the engine power decreases simultaneously so that there is not almost advantage in comparison with gasoline operation. If water-containing methanol is used and its water content, the suction pipe wall temperature and the ignition timing are suitable to reduce remarkably NO_x without lowering the power. Since in this case the concentration of aldehyde RCHO is considerably higher than that under gasoline operations, it is necessary to remove it through some appropriate measure.

2) The coefficient of cycle variation $S/\bar{P}_{max}$ in maximum combustion pressure has a minimum, about 5%, near $\lambda=0.85$.

Since, the value of $S/\bar{P}_{max}$ increases with increasing λ and when λ becomes larger than a certain value, it decreases.

In general, the value of $S/\bar{P}_{max}$ increases with increasing water content y and decreasing ignition advance θ but it decreases by heating the suction pipe and at the same time the combustible range also expands towards the leaner mixture side. In the case of $\lambda=1.2$, e.g., it is possible to improve $S/\bar{P}_{max}$ from 17 to 9% at t_w from 9 to 44℃, respectively.

3) $\bar{P}_{max}$ and $\Delta\bar{P}_{max}$, characteristics of the combustion pressure, as well as the flame velocity V_f take respective maximum near the excess air ratio $\lambda=0.85$ and at the same time their respective forming periods θ $(\bar{P}_{max})$, θ $(\Delta\bar{P}_{max})$ and the combustion duration θ_b have respective minimum. Since mixture burns more slowly with increasing λ, θ $(\bar{P}_{max})$, θ $(\Delta\bar{P}_{max})$ and θ_b increase, whereas $\bar{P}_{max}$, $\Delta\bar{P}_{max}$ and V_f decrease. At constant λ, $\theta(\bar{P}_{max})$, $\theta(\Delta\bar{P}_{max})$ and θ_b decrease and $\bar{P}_{max}$ and $\Delta\bar{P}_{max}$ increase with increasing suction pipe wall temperature, decreasing water content y and increasing ignition advance θ.

4) It is possible to observe positive strong correlations between $\bar{P}_{max}$ and $\Delta\bar{P}_{max}$, between $\theta(\bar{P}_{max})$ and $\theta(\Delta\bar{P}_{max})$ and between $S/\bar{P}_{max}$ and $\theta(\bar{P}_{max})$, whereas negative between $\bar{P}_{max}$ and $\theta(\bar{P}_{max})$ and between $\Delta\bar{P}_{max}$ and $\theta(\Delta\bar{P}_{max})$.

5) Although the mass rate of burning Y does not always coincide with the Wiebe's function, backward calculation of the characteristics number $\underline{m}$ with an experimental value Z $(\equiv\theta/\theta_b)$ at Y=0.5 reveals that the value of $\underline{m}$ decreases, within a range from 2.5 to 4.3, with increasing excess air ratio λ and ignition advance θ.

6) The maximum value of the rate of heat release $\left(\frac{d\bar{Q}}{d\theta}\right)_{max}$ are linearly proportional to $(H_u/M_o)/\lambda\theta_b$ and lie well on a straight line irrespective of gasoline or methanol operations.

This result coincides sufficiently with that of qualitative analysis by means of the Wiebe's function. A positive strong correlation exists between this $\left(\frac{d\bar{Q}}{d\theta}\right)_{max}$ and $\bar{P}_{max}$.

Nomenclatures

A	: Heat equivalent of work (Kcal/Kg·m)
CO	: Carbon monoxide concentration (%)
F	: Frequency of combustion pressure variation
G	: Flow rate (g/sec)
Hu	: Lower calorific value (Kcal/Kg)
Le	: Power (Ps)
Mo	: Theoretical Air/Fuel ratio (Kg/Kg)
N	: Engine speed (rpm)
NO_x	: Nitrogen oxide concentration (ppm)
$\bar{P}$	: Average combustion pressure at 1000 cycle (Kg/cm²)
$\bar{P}c$	: Average compression pressure (Kg/cm²)
P_{max}	: Maximum combustion pressure (Kg/cm²)
$\bar{P}_{max}$	: Average value of maximum combustion pressure (Kg/cm²)
ΔP	: Pressure difference the mean combustion and compression pressures (Kg/cm²)
$\Delta\bar{P}_{max}$	: Maximum value of pressure difference $\Delta\bar{P}$ (Kg/cm²)
$\bar{Q}$	: Quantity of heat release (Kcal)
$\bar{Q}_w$	: Quantity of emitted heat (Kcal)
RCHO	: Aldehyde concentration (ppm)
S	: Standard deviation
$S/\bar{P}_{max}$	: Coefficient of variation
THC	: Total hydrocarbon concentration (ppm)
t_e	: Exhaust gas temperature (℃)
t_w	: Suction pipe wall temperature (℃)
Vf	: Flame velocity (m/sec)
Y	: Mass rate of burning
y	: Water content (%)
η	: Thermal efficiency
η_v	: Volumetric efficiency
θ	: Crank angle (°CA)
θ_b	: Combustion period (°CA)
κ	: Specific heat ratio of mixture in the cylinder
λ	: Excess air ratio
a, m	: Characteristics numbers on the combustion

(Received May. 20, 1978)

References

(1) G. D. Ebersole : SAE Trans., 720692 (1972), Engine performance and exhaust emissions : Methanol vs. Iso-octane,

(2) E. J. Canton et al. : SAE paper 750698 (1975), Lean combustion of methanol-gasoline blends in a single cylinder SI engine,

(3) Kajitani et al. : Trans. Japan Soc. Mech. Engrs. Vol. 42, No. 360, (1976-8), A study of SI methanol engine,

(4) JIS K 0104 (1974), Methods for Determination of Oxides of Nitrogen in Exhaust Gases,

(5) G. M. Rassweiler : SAE Trans. 42-5 (1938), Motion pictures of engine flames correlated with pressure cards,

(6) Wiebe I. : Verlag der Akademie der Wissenschaften der UdSSR (1956),